Hydrodynamics of Gas-Agitated Liquid-Liquid Dispersions

Gas-agitated liquid-liquid dispersions arise in applications as diverse as direct hydrogenation processes for bitumen and coal, and the manufacture of iron and steel. The transfer of gas-phase constituents to the dispersed liquid phase and/or elution of dispersed-phase drops have been identified as potential limiting phenomena in these processes. Consequently, mean drop size and drop size distribution are key design variables. In this paper, the impact of gas flux and the physical properties of dispersed-phase constituents on the steady-state size distribution of liquid drops in lean liquid-liquid dispersions is quantified. The physical properties of the dispersed phase are shown to have a significant impact on drop size and drop-size distribution at low gas fluxes. Sauter mean drop size is correlated using theoretical models for drop break-up and coalescence. All results are compared with stirred tank analogues.

Savvas G. Hatzikiriakos
Rajendra P. Gaikwad
Philip R. Nelson
John M. Shaw
Department of Chemical Engineering
and Applied Chemistry
University of Toronto
Toronto, Ontario, Canada, M5S 1A4

Introduction

Phase interactions in gas-liquid, gas-solid and gas-liquid-solid systems have been the subject of numerous experimental and theoretical investigations (e.g., Kumar et al., 1976; Kato et al., 1976; Begovich and Watson, 1978; Hikata et al., 1980; Friedel et al., 1980; Kato et al., 1982). Phase interactions arising in gas-liquid-liquid systems, however, have received comparatively little attention, even though such three-phase systems can arise in hydrorefining processes (Shaw et al., 1988), pyrometallurgical processes such as copper convertors and the head boxes for continuously caste steel, and electro-organic synthesis.

Yoshida and Yamada (1972) measured the average diameter of kerosene drops dispersed in vertical tubes which were operated batchwise with respect to both liquids. The mean drop diameter was correlated with the power input per unit mass of liquid- and dispersed-phase concentration. The average drop size was found to be a function of power input (power input$^{-0.5}$) and to the volume fraction of oil (volume fraction$^{0.25}$). They also found that, for an equal mean drop size, the power consumption for a vertical tube was much less than that for agitated vessels, apparently substantiating their claim that bubble columns are more efficient contactors for liquid-liquid systems than mechanically agitated vessels. These authors did not vary the physical properties of the dispersed phase and did not report bubble size.

An empirical correlation relating mean drop size to column diameter and dispersed-phase viscosity was subsequently proposed by Hatate (1976). More recently, Kato et al. (1984) carried out experiments in a continuous, multistage bubble column with the kerosene-water-air system and correlated mean drop diameter as a function of superficial gas velocity, total liquid velocity and free area of a series of horizontal baffle plates. It is unclear in these latter instances whether the drop-size distributions were obtained at steady state or under dynamic conditions.

As potential applications for gas-liquid-liquid contactors can arise in systems with diverse physical properties and geometries, where the contactors may or may not be operated at steady state with respect to drop-size distribution, there is a need to focus investigations on fundamental interactions which affect mean drop size and drop-size distributions. In this paper, the impact of gas flux, dispersed-liquid-phase concentration and physical properties of dispersed-phase constituents on the steady-state size distribution of drops in lean liquid-liquid dispersions is quantified. Dynamic phenomena are addressed elsewhere (Hatzikiriakos et al., 1990).

Prediction of Mean Drop Size in Gas-Agitated Liquid-Liquid Dispersions

Isotropic turbulence approach

Kolmogoroff (1949) and Hinze (1955) independently suggested that the rate of energy dissipation in a flow is the key parameter characterizing the structure of turbulence fluctuations and hence drop size in turbulent liquid-liquid dispersions. Kolmogoroff identified velocity and length scales for the energy containing eddies. These eddies, eddies of the inertial subrange, are largely independent of both the large-scale geometry of flow and of the small-scale dissipative eddies. Since the functional role of these eddies is simply to convey energy upwards through the wave number spectrum, their structure is assumed to be the same for all flows with the same energy dissipation per unit mass, ϵ. Hinze (1955) predicted that drops and bubbles tend to break up in flow fields subject to isotropic turbulence if the Weber number exceeds unity, yielding:

$$d_{\max} \sim (\sigma/\rho)^{3/5}\epsilon^{-2/5} \tag{1}$$

Thomas (1981) adopted a similar approach and concluded that drop coalescence is probable if drop diameter is less than a minimum stable drop diameter, $d_{\min}$, defined as:

$$d_{\min} \sim 2.4\{\sigma^2 h^2/\mu_c \rho\epsilon\}^{1/4} \tag{2}$$

Equations 1 and 2 have been employed extensively in correlations for sauter mean diameter of dispersed-phase drops in mechanically-agitated liquid-liquid systems (Nishikawa et al., 1987; Coulaloglou and Tavlarides, 1976; Stamatoudis and Tavlarides, 1985), where they are coupled empirically with the effect of relative viscosity (μ_d/μ_c) (Hinze, 1955; Calderbank, 1967). The empirical model developed by Nishikawa et al. (1987), for a high shear impeller, is compared with the model proposed below.

Proposed model

The direct application of such correlations to gas-agitated dispersions is questionable, as the hydrodynamics of gas-agitated and mechanically-agitated vessels are fundamentally different. In mechanically-agitated vessels, for example, fluid is exposed to progressively higher shear rates as the energy dissipation rate (impeller speed) is increased, whereas in gas-agitated vessels, the maximum shear rate remains fixed unless the structure of the flow changes. This is particularly true for vessels operated in the bubbling flow regime where the impact of gas flux on bubble properties is modest. As the zone of greatest shear arises adjacent to rising bubbles, close scrutiny of individual bubble drop interactions provides an alternative basis for the prediction of dispersed-liquid-phase drop size at steady state.

In order for drops to become unstable in a shear field, we have from Hinze (1955)

$$\tau > \sigma/d + \{\mu_d/d\}\{\tau/\rho_c\}^{1/2} \tag{3}$$

where

$$\tau \sim \text{force/area} \sim \text{energy/volume}$$

On a microscopic level we can consider a single bubble-drop interaction, with a prevailing energy dissipation rate, ϵ, in the continuous fluid in the region of the rising bubble, and with a characteristic duration, t. Only a fraction of the available energy can be dissipated by the dispersed phase through internal circulation or through the creation of additional interfacial area. Much of the energy has an inappropriate length scale and merely causes drops to convect. Thus, we may write

$$\epsilon_{\text{eff}}\rho_c t > \sigma/d_{vs} + \mu_d/d_{vs}\{\epsilon_{\text{eff}} t\}^{1/2} \tag{4}$$

The effective energy per unit volume, $\epsilon_{\text{eff}}\rho_c t$, can be expressed as a function of the energy per unit volume of fluid per collision, the probability that a bubble will cause a drop to rupture and the energy fraction available for drop rupture. Each of these terms can be obtained by applying fundamental fluid mechanic concepts to the behavior of individual bubbles and drops.

Energy per Unit Volume per Collision. A differential energy balance for bubbles between the bottom and the top of a gas-agitated vessel can be used to estimate the average rate of energy dissipation. If the changes in kinetic and surface energy of the bubbles are neglected, the average power dissipated per unit mass in the vessel becomes:

$$\epsilon = \Delta\rho g(1 + \phi)U_g/\rho \tag{5}$$

Equation 5 is frequently approximated as:

$$\epsilon \approx gU_g \tag{6}$$

In the vicinity of a rising bubble, the superficial gas velocity approaches the bubble velocity, U_b, and the acceleration of fluid around the rising bubble, 4.5 U_b^2/D, approaches $3g$ for both ellipsoidal and spherical cap bubbles (Clift et al., 1978). The duration of an interaction can be approximated as the time required for a drop to go around a rising bubble, $\pi D/2U_b$. Thus,

$$\text{Energy per Unit Volume per Collision} \approx 1.5\pi\rho_c gD \tag{7}$$

Probability of a Bubble Causing a Drop to Rupture. The probability that bubbles will cause drops to rupture as they rise through a vessel can be expressed as the product of the number of collisions and the probability that a collision will lead to rupture. The probable number of collisions is obtained as the ratio of the time spent by an individual bubble in the vessel to the time between complete surface coverage, by bubbles, at a single elevation:

$$\text{No. of Collisions} = 1.5U_gH/DU_b \tag{8}$$

In the case of the rectangular vessel described in this work, a minimum superficial gas velocity of 0.0035 m/s is required to ensure that each drop is engaged in at least one collision event over this time period. The probability that a collision leads to drop rupture can be experssed as t/t^* where t is the duration of a collision event and t^* is the time required for the bubble and drop to approach to a distance, h, at which rupture occurs. t^* can be approximated from the classic lubrication problem where two equal-sized disks are pressed together with a constant force (Thomas, 1981):

$$t^* = 3\mu F d^2/\{32\pi\sigma^2 h^2\} \tag{9}$$

As the bubble and drop surfaces deflect similarly during the approach,

$$4\pi s^2 = Fd/\sigma = F'D/\sigma' \tag{10}$$

Eq. 9 becomes:

$$t^* = 3\mu F'Dd/\{32\pi\sigma\sigma' h^2\} \quad (11)$$

and the probability that a bubble will cause a drop to rupture becomes:

$$P = \{8\pi^2 U_g H\sigma\sigma'/D\mu U_b^2\}\{h^2/F'd\} \leq 1 \quad (12)$$

The distance from the bubble at which drop rupture occurs, h, and the force pushing the bubble and drop together, F', are both expected to decrease with drop size, but cannot be measured directly. Consequently, the experssion $h^2/F'\ d$ is treated as a parameter, C, in the model.

Energy Fraction Available for Drop Rupture. The energy associated with a bubble-drop interaction, Eq. 7, arises in the boundary layer surrounding a rising bubble. This boundary layer has a thickness, T, which is of the order of

$$T \approx D/Re^{1/2} \quad (13)$$

if potential flow is assumed, and internal recirculation of the bubbles is ignored. Under creeping flow conditions, the boundary layer thickness is three times greater for bubbles, as the velocity gradients adjacent to rising bubbles are substantially reduced.

The specific energy available in the boundary layer can be expressed in terms of the energy spectrum. All of this energy can be presumed to be available if drop diameter exceeds the boundary layer thickness, yielding:

$$1.5\pi g D = \int_{k(T)}^{\infty} E(k)\,\partial k \quad (14)$$

This approximation arises because velocity gradients in the wake (if present) are small. If drop diameter is less than the boundary layer thickness:

Energy Fraction Available for Drop Rupture

$$= \int_{k(d_{vs})}^{\infty} E(k)\,\partial k \Big/ \int_{k(T)}^{\infty} E(k)\,\partial k \quad (15a)$$

$$\approx \{d_{vs}/T\}^a \quad (15b)$$

as eddies larger than the drop cause convection and not drop rupture. The latter approximation, Eq. 15b, is possible because of the relative simplicity of the integral form of the energy spectrum when expressed as a ratio. In addition, the wave number is approximately proportional to the inverse of eddy diameter, if the eddies contained in the boundary layer are assumed to move at approximately the same mean speed with respect to the bulk liquid. The coefficient, a, varies continuously across the energy spectrum in the inertial subrange $a = 2/3$, whereas at higher wave numbers (small eddies) $a = 6$ or more. Only small eddies can arise in the boundary layer associated with bubbles, and the coefficient, a, is set at 6 in the model. The value of the coefficient, a, can also be estimated by comparing the size of the smallest eddies which might arise with the mean drop size obtained experimentally, following the approach of Thomas (1981). Such a calculation is approximate. However, mean drop size and eddy size are comparable, and the choice of a is further justified. See Schlichting (1979) for a more complete discussion of energy spectra.

Thus the proposed model for predicting steady state mean drop size in the absence of coalescence in gas agitated liquid-liquid dispersions, equation 16, is implicit and statistical in nature. This equation differs fundamentally from those proposed for mechanically agitated vessels, where vessel geometry plays such a key role. Liquid height and mean bubble diameter are the only reactor specific terms in equation 16.

$$\tau = 1.5\pi\rho_c g D\{8\pi^2 C U_g H\sigma\sigma'/D\mu U_b^2\} \leq 1 \cdot \{d_{vs}/T\}^6 > \sigma/d_{vs} + \{\mu_d/d_{vs}\}\{\tau/\rho_c\}^{1/2} \leq 1 \quad (16)$$

Drop-drop coalescence

The impact of drop-drop coalescence on mean drop size can be estimated from the probability of binary, ternary and quaternary collisions, which in turn are functions of dispersed-phase concentration. Higher-order terms may be neglected. As slip velocities for drops are low, drops must be in close physical contact before coalescence can occur. If each drop is assigned a cubic cell in a dispersion, interactions with six face neighbors and 12 edge neighbors must be considered. The probability that two drops are within a distance L' can be approximated as a sum of joint probabilities, P_2 for the two types of interactions:

$$P_2 \approx 6d_{vs}[L' + d_{vs}]/[L + d_{vs}]^2 + 3d_{vs}^2[L' + d_{vs}]^2/[L + d_{vs}]^4 \leq 1 \quad (17)$$

where

$$L + d_{vs} = d_{vs}[\pi/6\phi]^{1/3}$$

is the dimension of the cell. Similarly, the probability of a ternary interaction within a fixed distance can be expressed as:

$$P_3 \approx 2.25 d_{vs}^2[L' + d_{vs}]^4/[L + d_{vs}]^6 \leq 1 \quad (18)$$

and a quaternary interaction as:

$$P_4 \approx 0.1875 d_{vs}^2[L' + d_{vs}]^6/[L + d_{vs}]^8 \leq 1 \quad (19)$$

Mean drop diameter becomes a function of mean diameter at infinite dilution, i.e., d_{vs} from Eq. 16, and the incremental probability terms:

$$d_{vs\phi} \approx d_{vs}[1 + P_2(\sqrt[3]{2} - 1) + P_3(\sqrt[3]{3} - P_2\sqrt[3]{2}) + P_4(\sqrt[3]{4} - P_3\sqrt[3]{3})] \quad (20)$$

where the probabilities are evaluated in the limit $L' \rightarrow 0$, and each term in the sum is the product of the probability of the interaction type and the resultant increment in drop diameter.

Experimental Studies

Experiments were conducted in a vessel with a rectangular cross-section of 0.15 × 0.30 m. The vessel, 1.00 m in height, was constructed of 6.35-mm-thick sheets of perspex. Five taps of 12.7 mm diameter were drilled along the length of the column at 0.10 m intervals so that the pressure drop could be measured. five holes were also drilled in the bottom plate of the column and fitted with interchangeable nozzles (1.5, 2.5, 3.5 and 5.0 mm diameter). These holes linked the reactor to a gas chamber with a rectangular cross-section of 0.30 × 0.40 m and height of 0.40 m. The latter two features permitted bubble generation at constant pressure (Tsuge and Hibino, 1982), intermediate (Tsuge and Hibino, 1982), and constant flow (Wraith, 1971) conditions. Bubble size was varied at constant gas flux. Supplementary experiments were performed with a tubular reactor (0.3-m-dia., and 3-m-high, equipped with five 0.0025 m nozzles). Drop and bubble diameters were determined photographically using a Nikon camera (shutter speed 0.004 s) in conjunction with an image analyzer (Bausch and Lomb, Omnicon-3000 with NOVA-4 data general). A more detailed description of the apparatus and procedures can be found elsewhere (Hatzikiriakos et al., 1988).

The vessels were operated in batch mode with respect to both liquid phases. During a typical experiment, the vessels were filled with distilled water to a depth of 0.80 and 1.5 m, respectively, and saturated air was passed through the nozzles. The dispersed-phase liquid was introduced from the top through nozzle distributors with variable orifice diameters (3.2, 1.6, 1.0 mm). The initial drop sizes fell within the range 2,000 μm $< d <$ 10,000 μm. At low gas fluxes, photographs were taken while the column was operating. At higher gas fluxes, it was necessary to interrupt gas flow and photographs were typically taken only after 30 minutes of column operation. The experimental sauter mean drop diameter was obtained from Eq. 21.

$$d_{vs} = (\Sigma n_i d_i^3 / \Sigma n_i d_i^2) \tag{21}$$

where n_i is the number of particles within the diameter interval with a mean diameter d_i. The effects of superficial gas velocity, dispersed-phase volume fraction, interfacial tension, dispersed-phase viscosity and density were investigated independently using four liquid-liquid systems. The properties of the liquid-liquid systms are summarized in Table 1.

Results and Discussion

Gas holdup

The relationship between gas holdup and superficial gas velocity in the rectangular vessel is shown in Figure 1. The gas holdup in the range of 0.001–0.04 m/s for linseed oil + TCE-water-air and cottonseed oil + TCE-water-air is comparable to values given by Abou-El-Hassan (1979), who devised a generalized correlation for gas holdup in gas-liquid as well as gas-liquid-solid bubble columns. The presence of a dispersed phase leads to a reduction in gas holdup *vis-à-vis* corresponding gas-liquid systems. Kato et al. (1984) found that gas holdup in gas-liquid-liquid systems tended to be 10 to 15% lower than values encountered in gas-liquid systems. However, their correlation severely underestimates gas holdup at low gas fluxes. Kato et al. (1972) and Nakamura (1978) observed a similar reduction in gas holdup in bubble columns containing suspended solid particles *vis-à-vis* corresponding gas-liquid systems. This reduction in gas holdup has been attributed to an increase in the apparent viscosity of the bulk liquid resulting from the presence of a dispersed phase (Abou-El-Hassan, 1979) and would appear to be independent of the physical properties of the dispersed phase. Results obtained as part of this study, with a radically different geometry, are consistent with these findings.

Table 1. Physical Properties of Liquid-liquid Systems

System	μ_d, kg/m · s	σ, N/m	ρ_d, kg/m^3
A. Linseed Oil (85 vol.%) + TCE Water-Air	0.017	0.0062	1,000
B. Linseed Oil (96 vol. %) + TCE Water-Air	0.025	0.0061	950
C. Cottonseed Oil (83 vol.%) + TCE Water-Air	0.019	0.0236	1000
C. Dibenzyl Ether-Water-Air	0.005	0.0050	1040
E. Castor Oil (90 wt.%) + TCE	0.180	0.0343	1010

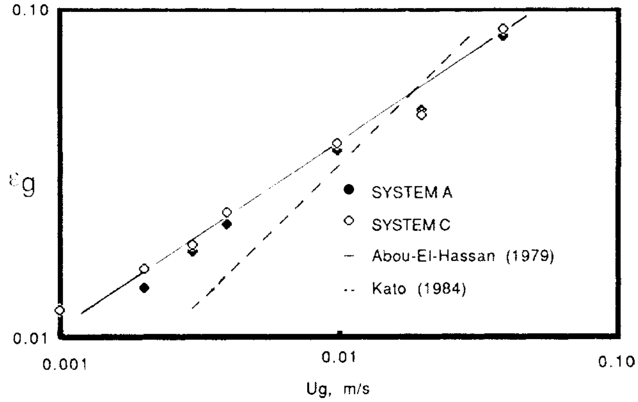

Figure 1. Gas holdup in three-phase systems.

Drop size distribution at steady state

Typical steady-state drop-size distributions are illustrated in Figure 2. These distributions, based on more than 1,000 drops per distribution, are approximately Gaussian. Similar distribu-

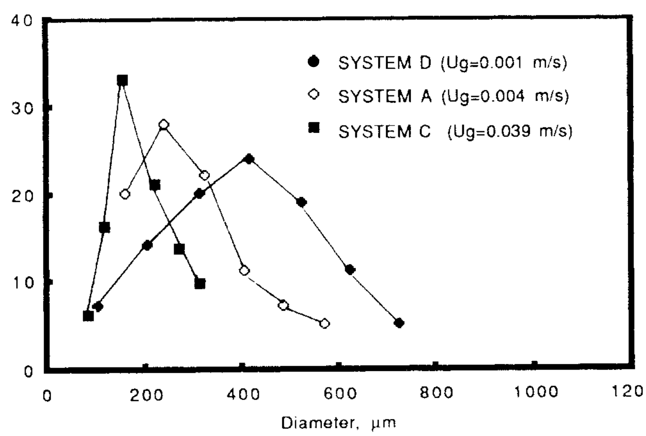

Figure 2. Sample size distributions for dispersed-phase drops.

tions have been reported for kerosene-water dispersions in mechanically-agitated vessels (Stamatoudis and Tavlarides, 1985). Drop-size distributions, under dynamic conditions, were investigated and are reported separately (Hatzikiriakos et al., 1990). During a typical experiment with system A, size distributions were obtained after 3, 10, 15 and 30 minutes (Figure 3). The large drops initially present were rapidly broken up, and steady-state size distribution profiles were obtained within 15 minutes as shown in Figure 3.

Variables Influencing Drop Size and Size Distribution at Steady State

Energy dissipation rate

Figure 4 shows the effect of energy dissipation rate, defined by Eq. 6, on the steady-state sauter mean diameter of dispersed liquid drops for three vessel geometries. Two flow regimes, one below and one above ~0.04 m^2/s^3 are clearly delineated for the results obtained with the rectangular vessel. As noted above, such a transition can be attributed to the probable number of bubble-drop collisions per drop arising in the vessel as a bubble passes through. The number of such collisions becomes unity at an energy dissipation rate of 0.035 m^2/s^3. Drop size distribution, as well as mean drop diameter, is affected by changes in energy dissipation rate, as shown in Figure 5. The range of stable drop sizes narrows as the superficial gas velocity is increased. This suggests that at high energy dissipation rates a dynamic equilibrium between coalescence and break-up may arise. A similar dependence is noted for mechanically-agitated vessels (Stamatoudis and Tavlarides, 1985).

Interfacial tension

Interfacial tension has a limited influence on mean drop diameter as shown in Figure 4. Systems A and C, for example, have approximately the same viscosity but their interfacial tensions differ by a factor of four. The effect of interfacial tension on mean drop size is less than anticipated by the equations of Thomas and Hinze which are based on isotropic turbulence. This difference can be attributed to the efficiency and modes of energy transfer to the dispersed phase in gas-agitated dispersions which do not conform with conditions prevalent in isotropically turbulent flow fields, i.e., the dominant role played by the viscous term in Eq. 16.

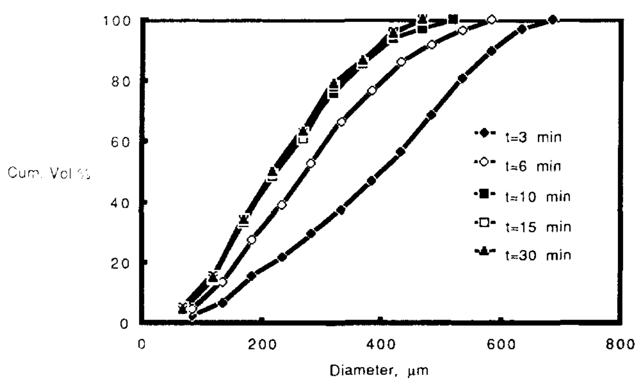

Figure 3. Dynamic drop-size distributions for system A, $Ug = 0.02$ m/s.

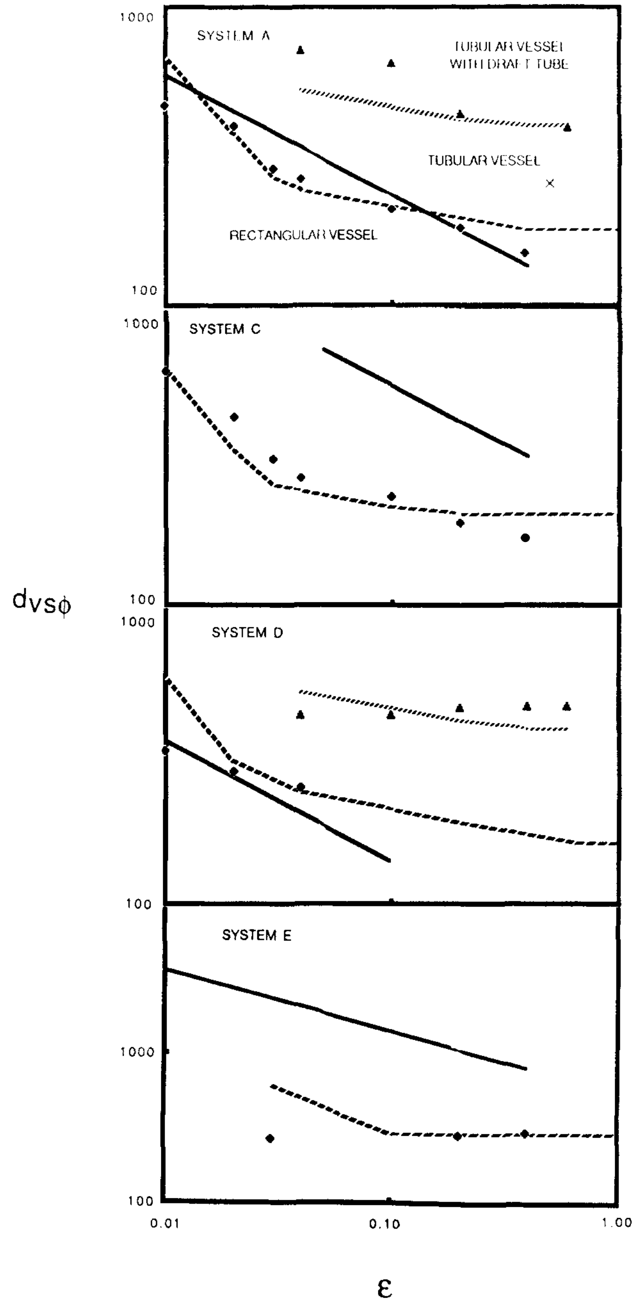

Figure 4. Effect of energy dissipation rate on mean diameter of dispersed-phase drops.

Equation 20 with the boundary layer thickness estimated from potential flow (---) and creeping flow (.......); Eq. 22 with $d_a/D' = 0.5, \phi = 0.0045$ (—)

Dispersed-phase concentration

The effect of dispersed-phase concentration on sauter mean diameter is shown in Figure 6. Sauter mean diameter tends to increase with dispersed-phase concentraiton over the range investigated. Limited dependencies, however, have been reported previously for lean and dense liquid-liquid dispersions in mechanically-agitated vessels (Narshimhan, 1980; Nishikawa et al., 1987) and for dense gas-agitated liquid-liquid dispersions (Kato et al., 1984). The impact of dispersed-phase concentration on sauter mean diameter is well predicted by the proposed

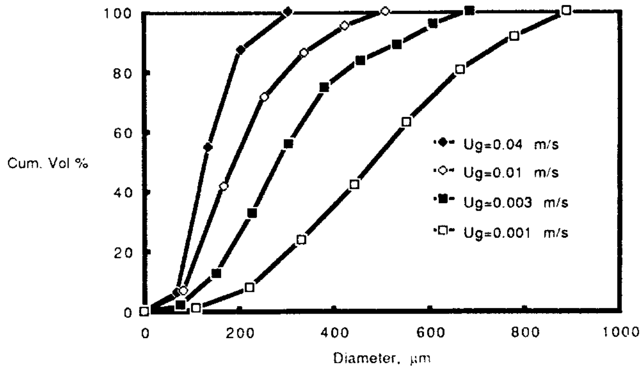

Figure 5. Breadth of drop-size distributions for system A.

model, Eq. 20, which suggests that mean drop size increases rapidly with concentration in the 0.5 to 3 vol. % range and then remains virtually constant up to concentrations exceeding 25%.

Relative viscosity

The steady-state sauter mean diameter is plotted against the relative viscosity at fixed interfacial tension in Figure 7. Superficial gas velocity is a parameter. The slopes of the experimental curves are related to the apparent power dependence of sauter mean diameter on viscosity. A power dependence of 0.256 was obtained by regression which conforms with the value, 0.25, obtained by Calderbank (1967) for bubble columns. Nishikawa et al. (1987) reported a power dependence ranging from 0.12 to

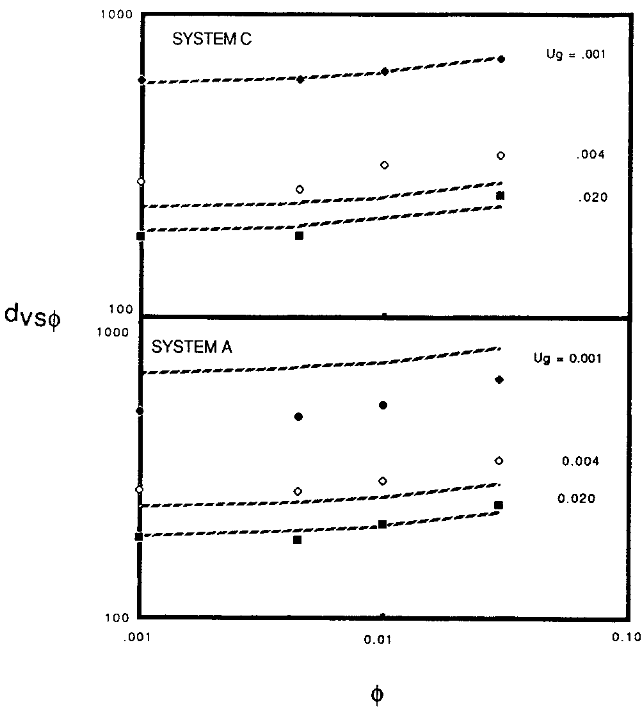

Figure 6. Effect of dispersed-phase concentration on Sauter mean diameter in a rectangular vessel.

Equation 20 with the boundary layer thickness estimated from potential flow (---)

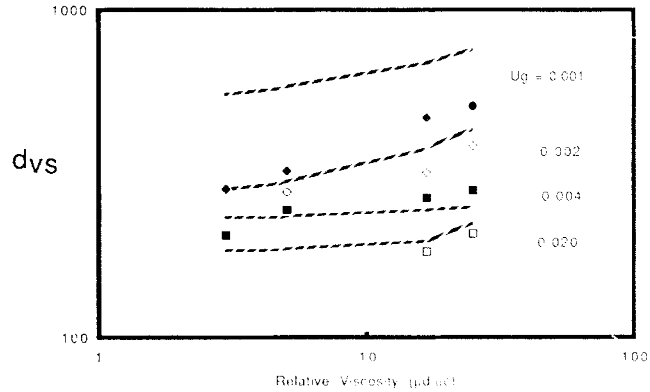

Figure 7. Effect of relative viscosity on the Sauter mean diameter of dispersed-phase drops in a rectangular vessel.

Equation 20 with the boundary layer thickness estimated from potential flow (---)

0.2 for mechanically-agitated vessels. The origin of the effect, however, may be seen more clearly with the proposed model, where the dependence on viscosity is a function of operating conditions and fluid properties.

Vessel geometry

Preliminary experiments performed with a tubular reactor indicate the same trends as observed in the rectangular vessel. However, the drops are larger, particularly in the presence of a draft tube as shown in systems A and D of Figure 4. This effect is attributed to the longitudinal recirculation imparted by the draft tube, which radically reduces the velocity gradients in the boundary layer surrounding rising bubbles. The observed mean drop sizes are consistent with a boundary layer thickness estimated from the creeping flow approximation and are modeled accordingly in systems A and D. In the absence of a draft tube, mean drop size in the tubular vessel lies between the creeping flow and potential flow extrema in system A. Thus the flow pattern of the continuous fluid as opposed to geometry *per se* has a significant influence on mean drop size. Since bubble boundary layer behavior is bounded by the creeping flow and potential flow assumptions, mean drop size can be predicted within 50% for a vessel of arbitrary shape. Even limited knowledge concerning the flow pattern of the continuous fluid reduces this error substantially, whereas the use of correlations designed for mechanically-agitated vessels can lead to unpredictable and large errors as shown on Figure 4.

Other parameters

The relative density of the dispersed and continuous phases had no effect on sauter mean diameter in the range $0.95 < \rho_{ld}/\rho_{lc} < 1.04$. Experimental data related to relative density in the range $1.04 < \rho_{ld}/\rho_{lc} < 1.13$ is inconclusive as far as the effect of relative density is concerned. However, little dependence is anticipated, see Eq. 16. Initial drop size has no effect on the steady-state sauter mean diameter for initial drop sizes in the range 2,000 μm $< d <$ 10,000 μm. Variation of mean bubble diameter, at constant gas flux, over the range 1.0 to 2.5 cm also had no apparent effect on mean drop diameter at steady state in the region where $d > T$ which also conforms with Eq. 16.

Verification of the Model

The dashed curves on Figures 4, 6 and 7 correspond to the model predictions with $C = 7.0 \times 10^{-4}\ s^2 \cdot kg^{-1}$, $L'/d = 0$, $a = 6$, and T defined by Eq. 13. The overall fit of the model is satisfactory for the diverse systems investigated, and it illustrates the appropriateness of the approach. Apart from the evaluation of C, no effort was made to optimize the fit of the model to the data or estimate the effect of physical properties/operating conditions on the value of the model parameters, as this would detract from the simplicity and generality of the model. Relaxation of the severe constraint imposed on L' in particular may improve the evaluation of the impact of concentration on mean drop diameter, which tends to be underestimated in the present model. Model predictions are also sensitive to the value of the boundary layer thickness, at high energy dissipation rates, and Eq. 13 can lead to slight over/under prediction of drop size under these conditions.

Model parameters do not appear to exhibit a strong apparatus dependence, as the dominant interactions typically remain individual drop-drop or bubble-drop interactions. Preliminary experiments, performed with tubular and rectangular vessels and shown on Figure 4 appear to confirm this finding. Additional experiments with alternative geometries are in progress and will be reported at a later date.

Comparison with Mechanically-Agitated Vessels

The relative performance of gas and mechanically-agitated vessels as contactors for liquid-liquid systems can be compared on the basis of energy consumed per unit of interfacial area. The results of this investigation are ocmpared with those of Nishikawa et al. (1987), who summarized the impact of operating parameters on the steady-state sauter mean diameter of dispersed-phase drops in vessels agitated with a high shear impeller as:

$$d_{vs\cdot a} = 0.105\epsilon^{-2/5}(d_a/D')^{6/5} (1 + 2.5\phi^{2/3})(\mu_d/\mu_c)^{13/40}(\sigma/\rho)^{3/5} \qquad (22)$$

Equation 22 fits their data well and agrees with other correlations associated with dispersion studies in mechanically-agitated vessels. The impact of power dissipation rate on the sauter mean diameter for gas- and mechanically-agitated vessels is illustrated for four different systems in Figure 4, with $d_a/D = 0.5$. For systems A and D, systems with a low interfacial tension, the sauter mean diameters obtained in gas- and mechanically-agitated vessels are comparable at low energy dissipation rates, in the absence of longitudinal recirculation. Mechanical agitation is preferred at higher energy dissipation rates. For systems C and E which possess high interfacial tensions, mean drop diameter is much greater in mechanically-agitated vessels than in gas-agitated vessels, particularly at low energy dissipation rates. The large mean diameters obtained in mechanically-agitated vessels, at low energy dissipation rates, can be attributed to coalescence in zones remote from the impeller (Mlynek and Resnick, 1972; Weinstein and Treybal, 1973). Such zones do not exist in gas-agitated dispersions, and in this latter case, gas-agitated vessels are preferred over a broad range of operating conditions. As the role of relative viscosity is comparable in both gas- and mechanically-agitated vessels, this parameter is of secondary importance for comparative purposes.

The comparative advantage of gas-agitated vessels is greatest for fluids with high interfacial tension (as the steady-state sauter mean diameter has only a limited dependence on interfacial tension), at low to moderate energy dissipation rates. The region of comparative advantage for gas-agitated vessels is further constrained if the flow of continuous fluid surrounding bubbles is "laminar," as drops tend to be large in this case. At steady state, each case must be assessed independently, and gas-agitated vessels are not preferable *a priori*. However, a comparison between gas-agitated and mechanically-agitated vessels operating under dynamic conditions shows that the former may be preferred for a broad range of liquid-liquid systems (Hatzikiriakos et al., 1990).

Conclusions

Gas-agitated and mechanically-agitated liquid-liquid dispersions exhibit fundamentally different hydrodynamic behavior at steady state, and neither reactor type is preferred in general. The mean drop size of dispersed-phase drops in gas-agitated liquid-liquid dispersions can be expressed as a function of the physical properties of dispersed phase, bubble boundary layer thickness, and energy dissipation rate. Dispersed-phase properties have the greatest impact on mean drop size at low energy dissipation rates whereas boundary layer thickness becomes increasingly important at higher energy dissipation rates. Steady-state mean drop diameters in gas-agitated vessels can be less than, equal to, or greater than mean drop diameters arising in mechanically-agitated vessels equipped with high shear impellers. As mean drop diameter is less dependent on interfacial tension in gas-agitated vessels than in mechanically-agitated vessels, the comparative advantage is greatest for two-phase liquids with high interfacial tensions. Gas-agitated vessels are also preferred for two-phase liquids with a high relative viscosity, at low energy dissipation rates.

Acknowledgment

The authors wish to acknowledge grants received from the Natural Science and Engineering Research Council, the Bickell Foundation and the University of Toronto, without which this work could not have been performed.

Notation

a = dimensionless exponent
C = dimensional constant, $s^2 \cdot kg^{-1}$
d, d_a = drop diameter, impeller diameter, m
d_{max}, d_{min} = maximum and minimum stable drop diameter, m
$d_{vs}, d_{vs\phi}, d_{vs\cdot a}$ = Sauter mean diameter: infinite dilution, concentration ϕ, agitated vessel, m
D, D' = bubble diameter, vessel diameter, m
E = frequency
F, F' = force acting on the drop, bubble, $kg \cdot m \cdot s^{-2}$
g = gravitational acceleration constant, $m \cdot s^{-2}$
h = critical rupture thickness, m
H = liquid depth, m
k = wave number
L, L' = average drop-drop distance, drop-drop distance, m
P_2, P_3, P_4 = coalescence probabilities
Re = Reynolds Number
s = radius, m
T = boundary layer thickness, m
t, t^* = time, characteristic time, s
U_g, U_b = superficial gas and bubble velocity, $m \cdot s^{-1}$

Greek letters

τ = shear stress, $kg \cdot m^{-1} \cdot s^{-2}$
$\kappa = \mu_d/\mu_c$
σ', σ = surface tension: gas continuous liquid, liquid-liquid, $kg \cdot s^{-2}$
ϵ = energy dissipation per unit mass, $m^2 \cdot s^{-3}$
ϵ_g = gas fraction of slurry
μ, μ_c, μ_d = liquid viscosity, viscosity of continuous and dispersed liquid phases, $kg \cdot m^{-1} \cdot s^{-1}$
$\rho\rho_c\rho_d$ = density of the bulk liquid, the continuous liquid, dispersed liquid, $kg \cdot m^{-3}$
$\Delta\rho$ = density difference between the liquid and gas phases, $kg \cdot m^{-3}$
ϕ = volume fraction of the dispersed phase in the liquid-liquid dispersion

Literature Cited

Abou-El-Hassan, M. E., "Mixing and Phase Distribution in Two- and Three-Phase Bubble Column Reactors," *Proc. Eur. Conf. on Mixing,* 303 (1979).

Begovich, J. M., and J. S. Watson, "Hydrodynamic Characteristics of Three-Phase Fluidized Beds," *Fluidization, Proc. Eng. Found. Conf.,* J. F. Davidson and D. L. Kairns, eds., 190 (1978).

Calderbank, P. H., "Gas Absorption from Bubbles," *The Chem. Engr.,* **45,** 209 (1967).

Clift, R., J. R. Grace, and M. E. Weber, *Bubbles Drops and Particles,* Academic Press, New York, Chs. 7 and 8 (1978).

Coulaloglou, C. A., and L. L. Tavlarides, "Drop Size Distributions and Coalescence Frequencies of Liquid-Liquid Dispersion in Flow Vessels," *AIChE. J.,* **22,** 289 (1976).

Friedel, L., P. Herbrechtsmier, and R. Steiner, "Mean Gas Holdup in Downflow Bubble Columns," *Ger. Chem. Eng.,* **3,** 342 (1980).

Hatate, Y., S. Mori, S. Okuma, and Y. Kato, "Drop Size in Gas-Liquid-Liquid System Bubble Columns," *Kagaku Kogaku Ronbunshu,* **2,** 133 (1976).

Hatzikiriakos, S. G., R. P. Gaikwad, and J. M. Shaw, "Characterization of Gas-Liquid-Liquid Tubular Reactors," AIChE Meeting, Paper 9F, New Orleans (Mar., 1988).

———, "Transient Drop Size Distributions in Gas Agitated Liquid-Liquid Dispersions," *Chem. Eng. Sci.,* in press (1990).

Hikata, H., S. Asai, K. Tanigawa, K. Segaga, and M. Kitao, "Gas Holdup in Bubble Column," *Chem. Eng. J.,* **20,** 59 (1980).

Hinze, J. O., "Fundamentals of the Hydrodynamic Mechanism of Splitting in Dispersion Processes," *AIChE J.,* **1,** 289 (1955).

Kato, Y., A. Nishigaki, F. Takashi, and S. Tanaka, "The Behaviour of Suspended Particles and Liquid in Bubble Columns," *J. Chem. Eng. Japan,* **5,** 112 (1972).

Kato, Y., A. Nishiwaki, S. Tanaka, and T. Fukuda, "Longitudinal Concentration Distribution of Suspended Solid Particles in Multi-Stage Bubble Columns," *J. Chem. Eng. Japan,* **15,** 376 (1982).

Kato, Y., T. Kago, and S. Morooka, "Longitudinal Concentration Distribution of Droplets in Multi-Stage Bubble Columns for Gas-Liquid-Liquid Systems," *J. Chem. Eng. Japan,* **17,** 429 (1984).

Kato Y., T. Kago, S. Morooka, and A. Nishiwaki, "longitudinal Dispersion of Droplet Phase in Single and Multi-Stage Bubble Columns for Gas-Liquid-Liquid Systems," *J. Chem. Eng. Japan,* **18,** 154 (1985).

Kito, M., M. Shimida, T. Sakai, S. Sugiyama, and C. Y. Wen, "Performance of Turbulent Bed Contactor, Gas Holdup and Interfacial Area Under Liquid Stagnant Flow," *Fluidization,* 411 (1976).

Kumar, A., T. T. Dagaleesan, G. S. Laddha, and H. E. Hoelscher, "Bubble Swarm Characteristics in Bubble Columns," *Can. J. Chem. Eng.,* **54,** 503 (1976).

Mlynek, Y., and W. Resnick, "Drop Sizes in an Agitated Liquid-Liquid Systems," *AIChE J.,* **18,** 122 (1972).

Nakamura, M., K. Hioki, A. Takahashi, H. Tanahashi, and S. Watari, "Fluid Flow Characteristics of the Three Phase Fluidized Bed with Perforated Plates," *Kagaku Kogaku Ronbunshu,* **5,** 473 (1978).

Narsimhan, G., D. Ramkrishna, and J. P. Gupta, "Analysis of Drop Size Distributions in Lean Liquid-Liquid Dispersions," *AIChE J.,* **26,** 991 (1980).

Nishikawa, M., F. Mori, and S. Fujieda, "Average Drop Size in a Liquid-Liquid Phase Mixing Vessel," *J. Chem. Eng. Japan,* **20,** 82 (1987).

Schlichting, H., *Boundary Layer Theory,* 7th ed., Ch. 17, McGraw-Hill, New York (1979).

Shaw, J. M., R. P. Gaikwad, and D. A. Stowe, "Phase Splitting of Pyrene-Tetralin Mixtures," *Fuel,* **67,** 1554 (1988).

Stamatoudis, M., and L. L. Tavlarides, "Effect of Continuous-Phase Viscosity on the Drop Sizes of Liquid-Liquid Dispersions in Agitated Vessels," *Ind. Eng. Chem. Process Des. Dev.,* **24,** 1175 (1985).

Thomas, R. M., "Bubble Coalescence in Turbulent Flows," *Int. J. Multiphase Flow,* **7,** 709 (1981).

Tsuge, H., and S. Hibino, "Bubble Formation from an Orifice Submerged in Liquids," *Chem. Eng. Commun.,* **22,** 63 (1983).

Weinstein, B., and R. E. Treybal, "Liquid-Liquid Contacting in Unbaffled, Agitated Vessels," *AIChE J.,* **19,** 304 (1973).

Wraith, A. E., "Two Stage Bubble Growth at a Submerged Plate Orifice," *Chem. Eng. Sci.,* **26,** 1659 (1971).

Yoshida, F., and T. Yamada, "Average Size of Oil Drops in Hydrocarbon Fermentors," *J. Ferment. Technol.,* **49,** 235 (1971).

Manuscript received July 31, 1989, and revision received Mar. 5, 1990.